JOURNAL OF COMPUTATIONAL PHYSICS 105, 14-23 (1993)

HECTOR: A Code for the Study of Charged Particles in Axisymmetric Tokamak Plasmas

M. A. KOVANEN* AND W. G. F. CORE

JET Joint Undertaking, Abingdon, Oxfordshire OX14 3EA, United Kingdom

Received November 7, 1990; revised April 27, 1992

A new charged particle orbit following code HECTOR is described. The code simulates the behaviour of thermal particles and high energy particles, such as those resulting from the ICRF wave field interactions or from thermonuclear reactions within the confining magnetic fields of non-circular axisymmetric tokamak plasmas. The particle trajectories are traced using a new, fast, and efficient hybrid orbit-following scheme, based upon the drift equations in the guiding centre approximation and the constants of motion. The Monte Carlo technique is used to describe the Coulomb scattering processes of dynamical friction, pitch angle scattering, energy diffusion, and the ICRF interaction processes. The code is specifically designed to operate within the experimental environment.

I. INTRODUCTION

The operation of large tokamaks (JET, TFTR) with substantial levels of additional heating or close to ignition conditions leads to the occurence of supra-thermal ion tails and of significant concentrations of fusion products within the plasma volume. These charged particles have energies in the million electron volt range, have long slowing down times which are typically 1 s in systems close to ignition, have large Larmor radii, and, especially for particles trapped in the toroidal field gradients, make large radial excursions across the minor cross section of the torus. Large banana-width particles will lead to a significant broadening of the heating profile and, in addition, can be produced on orbits that intersect the vessel wall or enter the "loss cone" through particle–wave interactions or through Coulomb scattering on the background plasma, leading to increased impurity production and wall loading. Furthermore, the escaping fast ions can provide important information on the auxiliary heating efficiency and thermonuclear activity within the discharge. A detailed knowledge of the particle trajectories is essential to the theoretical and experimental understanding of tokamak systems close to ignition. The common use of small banana-width approximations in these situations is highly questionable and may lead to serious erroneous results. An accurate description of the charged particle behaviour is therefore of primary importance for reactor feasibility studies and for diagnostic purposes.

A number of Monte Carlo codes or codes using the constants of motion (COM) method have been developed either to classify the orbit topology or to follow the guiding centres of charged particles moving in the magnetic field of a tokamak or similar plasma containment devices [1–16]. Many of the codes have only a limited number of applications, particularly those which relate to present-day experiments. The most severe problem, however, is that the time scale to find the heating and diffusion rates is so long that the numerical uncertainties often dominate any perceived physics, or the demand for the computational resources is so large that such codes are far too expensive for routine use in the predictive or experimental environment. It is clear that there is a pressing need for a fast code which can be used to address a number of important charged particle problems.

In this work we describe a procedure for tracing charged particle orbits in noncircular tokamak containment systems. The code was originally designed to study the behaviour of fast ions residing in the tail of distributions during heating in the ion cyclotron range of frequencies (ICRF) or resulting from fusion reactions within the discharge. However, many applications require an accurate description of the thermal particle behavior, and accordingly, a treatment of low energy particles is also included in the code. The consideration is restricted to systems exhibiting toroidal asisymmetry and includes the Coulomb scattering processes of dynamical friction, pitch angle scattering, and energy diffusion due to collisions with the background electrons and ions, and the resonant ion interaction with ICRF wave fields. A hybrid integration scheme based upon the drift equations in the guiding centre approxima-

* Lappeenranta University of Technology, Lappeenranta, Finland and National Research Council for Technology, The Academy of Finland, Helsinki, Finland.

0021-9991/93 $5.00

tion and upon the COM method is used to follow the test particles. In this numerical technique, the problem of error accumulation is avoided. The invariance of the toroidal canonical angular momentum enables arbitrarily large integration steps to be used, and particle trajectories obtained in this way remain close to the actual orbit throughout the integration.

The structure of this work is as follows. In Section II, the methods for the investigation of charged particle behaviour in the confining magnetic field of a tokamak plasma are reviewed and their areas of application discussed. In Section III, the Monte Carlo model operators describing the Coulomb collision and ICRF interaction processes are presented. Then, in Section IV the procedure for mapping the charged particle source distribution from the local phase space coordinates to the COM system is described, and in Section V, the code input data specification and modes of operation are detailed. Finally, the test results are presented in Section VI.

II. METHODS FOR THE INVESTIGATION OF CHARGED PARTICLE TRAJECTORIES

In this section we first review current methods and areas of application for tracking charged particles in tokamak containment systems. Then a new method based upon the drift equations in the guiding centre approximation and the constants of motion is described. The coordinate system used is shown in Fig. 1.

(i) *Full Orbit Calculation*

The full equation of motion for charged particles is

$$m\dot{\mathbf{v}} = q(\mathbf{E} + \mathbf{v} \times \mathbf{B}),$$

where m is the particle mass, $\mathbf{v}$ is the particle velocity, q is the particle charge, and $\mathbf{E}$, $\mathbf{B}$ are the electric and magnetic fields, respectively.

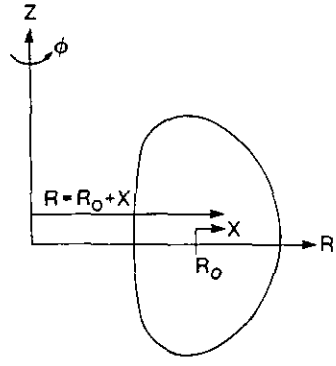

FIG. 1. (R, ϕ, Z)-coordinate system.

The advantage of using the exact equation is its accuracy in describing the orbits. However, calculations of this type, besides having numerical error accumulation, are time consuming and not well suited to simulation studies, where a large number of particle trajectories are to be examined. Consequently, the full orbit representation is limited to situations where detailed information on the actual gyromotion is required, such as for orbits of heavy ions with low charge state.

(ii) *Guiding Centre Approximation*

The velocity components of the guiding centre motion are readily obtained from the collisionless drift equations. We have

$$\mathbf{v}_{g.c.} = v_{||}\mathbf{b} - v_{||}\mathbf{b} \times \nabla\left(\frac{v_{||}}{\omega_{ci}}\right),$$

where the component of the guiding centre velocity projected along the magnetic field line is $v_{||} = \pm[2(E - \mu B/m]^{1/2}$, $\mathbf{b} = \mathbf{B}/|\mathbf{B}|$ is the unit vector in the direction of the magnetic field, $\omega_{ci} = qB/m$ is the ion cyclotron frequency, $E = \frac{1}{2}mv^2$ is the particle energy, $\mu = \frac{1}{2}mv_{\perp}^2/B$ is the magnetic moment, and v, $v_{\perp}$ are the magnitude and perpendicular component of the particle velocity, respectively.

Whatever numerical integration method is used for the guiding centre equation there are two severe problems. The first is the accumulative numerical error which limits the integration step length to 10–20 times the step length used with full orbit calculations. To be able to simulate thousands of slowing down orbits, a greatly enhanced numerical acceleration ($> 10^3$) of the slowing down processes must be introduced leading to a distorted orbit topology. The effect of numerical error accumulation on a typical orbit is shown in Fig. 2. It is to be noted that the error in the flux coordinate appears to grow almost linearly with the integrated orbit. The second problem is the turning point where $v_{||}$ changes sign. To implement a long integration step procedure the calculation of the actual coordinates of the orbit turning point, where $v_{||} = 0$, can require a considerable investment in interpolation and, consequently, a significant fraction of the computational time. In the following section, a method of orbit integration is described which surmounts these difficulties.

(iii) *Drift Equation and Constants of Motion Approximation Hybrid Method*

In the absence of interacting processes three constants of motion, the particle velocity v, magnetic moment μ, and toroidal canonical angular momentum P_{ϕ} completely characterise the guiding centre motion of charged particles moving within the confining magnetic fields of a axi-

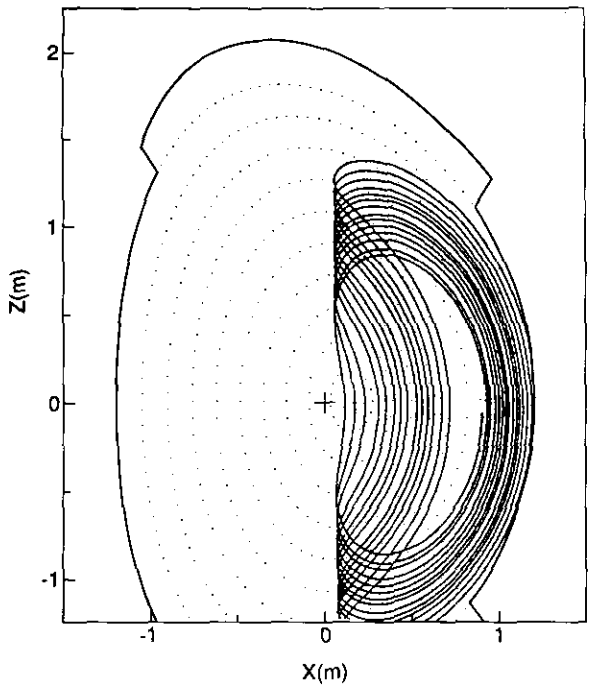

FIG. 2. Effect of the accumulative numerical error on a collisionless α-particle orbit calculated using the guiding centre approximation.

symmetric tokamak. In systems having arbitrary cross section [17]

$$P_\phi = mRv_{||}B_\phi/B - q\psi,$$

where $B=(B_R^2+B_\phi^2+B_Z^2)^{1/2}$, and ψ is the poloidal flux function.

If a simple formula for ψ is used, the spatial coordinates of the charged particles can easily be solved. This, however, represents only a small minority of cases relevant to present-day tokamaks. In the general situation ψ is obtained either as a numerical solution of the Grad–Shafranov equation for plasma equilibria or as a fit to the experimental magnetic measurements. Thus, an alternative method to find the spatial coordinates has to be used. This is usually done by writing the set of (P_ϕ, μ, v) invariants as a function of R and ψ and by assuming $B=B_\phi$ [16]. The (R, Z) coordinates can then be obtained by a one-dimensional interpolation of ψ. The resulting orbit error, when compared with the case where the poloidal magnetic field component B_θ is included, is small if the plasma current is low [18] but will become significant for discharge currents in the present large tokamaks currently operating (JET, TFTR) or in future igniting tokamaks.

To include B_θ the interpolation has to be done in a two-dimensional (R, ψ) space. This is done in HECTOR with a hybrid integration technique which combines the drift equations and the COM method. First, a long single guiding centre step is taken to give predicted spatial coordinates $(R, Z)_{g.c.}$. Then, coordinates $(R, Z)_\perp$ are chosen perpendicular to the line between the predicted and previous orbit coordinates. The actual coordinates that satisfy $P_\phi=$ constant can then be easily found by linear interpolation between $(R, Z)_{g.c.}$ and $(R, Z)_\perp$. An example of a first orbit obtained with this method is shown in Fig. 3. The drift equation gives the optimum predicted spatial coordinates and, consequently, increases the overall efficiency of the integration procedure. The sign of $v_{||}$ is automatically included in the integration, and numerical error accumulation and the problem of locating the spatial coordinates of the turning points are avoided.

The location on the orbit, where the particle undergoes the ICRF interaction is determined from the resonance condition

$$B=\frac{m}{nq}(\omega - k_{||}v_{||}),$$

where ω is the frequency of the wave field, $k_{||}$ is the parallel wave number, and n is an integer. After the particle has crossed this value of magnetic field, the spatial coordinates are corrected to take into account the resonance duration time and the subsequent changes in the (P_ϕ, μ, v) coordinates using the ICRF model operator, which is described in Section III.

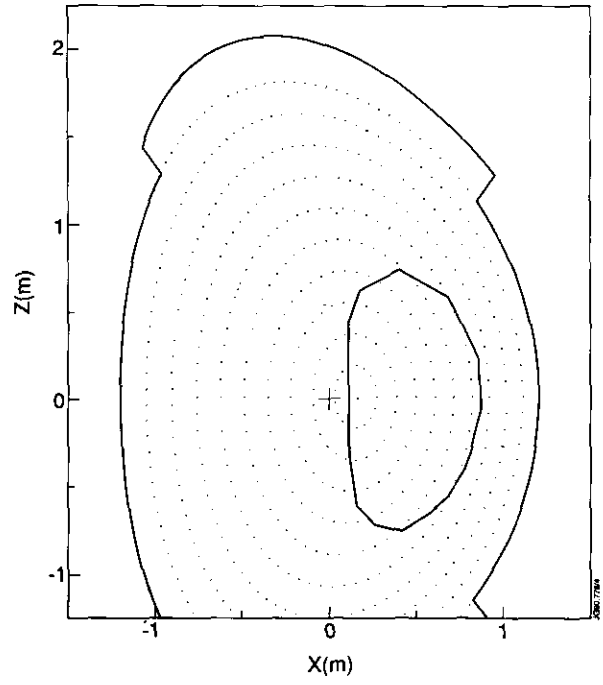

FIG. 3. Typical collisionless 3.5 MeV α-particle orbit traced using long (4 m) integration steps with the hybrid method. It is seen that even with this large integration step the orbit remains closed.

The integration step length is in the usual form

$$\Delta t = \frac{\Delta s}{v}\left[1 + a\mu\left(\frac{2B}{mv^2}\right)\right].$$

Goldston *et al.* [10] used $a = 1.5$, but to increase the accuracy of the orbits of deeply trapped particles $a = 1.0$ is chosen here. This is particularly important for the simulation of anisotropic minority ion distributions produced during ion cyclotron resonance heating (ICRH). It is to be noted, that for a given pitch angle the spatial integration steps do not depend on the particle energy. Furthermore, the poloidal steps become shorter when the cosine of the pitch angle or the poloidal field value decreases. Thus, a constant number of integration steps per bounce orbit can be roughly maintained independent of the particle energy, pitch angle, or radial position. For such calculations as ICRH, the decrease in the poloidal step length for particles moving close to the plasma centre leads to improved accuracy. Typically the step-size Δs is 1–2m. Because of the increase in the poloidal step length as the particle moves through the outer region of the plasma, Δs is reduced to ~ 0.5 m to obtain accurate results for the heat and particle distributions on the wall. This is particularly important for studies of flows in the X-point region.

Computing particle trajectories is time consuming, but the use of the hybrid method can reduce this time significantly. As a specific example, to obtain a $\sim 1\%$ error in the radial coordinates of a collisionless 3.52 MeV α-particle orbit after a Spitzer time, the step length using the Runge–Kutta method [19] has to be in the region of three orders of magnitude shorter than that used in the hybrid scheme. Although the interpolation in the hybrid method involves a considerable computation time, this method can still reduce the CPU time by a factor of >25. When the collisions are included the optimising of the CPU time depends, further, on the efficiency of the scattering operators (Section III), on the way the scattering processes are accelerated (Section III), and on the speed of the data handling routines which provide local plasma parameters along the trajectory (Section V). To calculate the α-particle slowing down orbits from the initial energy of 3.52 MeV to the thermal energy takes typically ~ 100 h/1000 particles on the CRAY computer. To reduce this large CPU time a number of fast orbit following codes have recently been developed, such as that in Ref. [20] which achieved a speed up factor of ~ 20. To obtain a significant reduction in the CPU time, approximations have to be used. This limits the range of application and in many cases can lead to serious departure from the actual physics under investigation. This is avoided by using the hybrid orbit integration technique combined with efficient routines for scattering, acceleration, and data handling, and a substantial saving in CPU time is gained. A simulation of 2000 α-particle slowing down orbits with HECTOR takes 10–15 min on the IBM-3090-300J computer, and creating an energetic tail in the minority ion distribution function from an initially thermal population with ICRH takes ~ 20 min/2000 particles.

Extensive tests, which are described later in Section VI, demonstrate the validity of the code. Although the hybrid method can only be applied to tokamaks with toroidal magnetic axisymmetry, the ripple amplitude in the current large tokamaks is small and can be neglected.

III. SLOWING DOWN AND ICRF-INTERACTION PROCEDURE

The inclusion of the effects of Coulomb scattering and ICRF interaction on the particle trajectories is straightforward and conceptually simple. Collisions are taken into account by calculating new values of the particle velocity, magnetic moment, and toroidal canonical angular momentum after each time step. We have

$$v \to v + \Delta v$$

$$\mu \to \mu + \Delta\mu$$

$$P_\phi \to P_\phi + \Delta P_\phi,$$

where

$$\Delta\mu = \frac{m}{2B}\left(2v\,\Delta v + \Delta v^2 - 2v_{\|}\,\Delta v_{\|} - \Delta v_{\|}^2\right)$$

and

$$\Delta P_\phi = mRB_\phi\,\Delta v_{\|}/B$$

are the incremental changes in the magnetic moment ($\Delta\mu$) and toroidal canonical angular momentum (ΔP_ϕ) due to the accumulative effects of dynamical friction, pitch angle scattering, energy diffusion, and particle wave interaction occurring during the time step. Δv and $\Delta v_{\|}$ are the incremental changes in particle velocity and its parallel component, respectively. The usual inclusion of only the first-order terms in $\Delta\mu$ leads to accumulative error in μ and, consequently, to a loss of energy conservation. This is avoided here by the use of the second-order differentials in $\Delta\mu$.

(i) *Friction*

Following the analytical treatment of the Fokker–Planck equation by Stix [21], one can write the change in particle velocity occurring during a time interval Δt as

$$\Delta v = -\sum_f \left(C_f \frac{m}{2kT_f} G(l_f v)\,\Delta t\right),$$

where

$$C_f = 8\pi n_f Z_f^2 Z^2 e^4 \ln \Lambda / m^2$$

$$l_f^2 = m_f/(2kT_f)$$

$$G(x) = \frac{\phi(x) - x\phi'(x)}{2x^2}$$

$$\phi(x) = \frac{2}{\pi^{1/2}} \int_0^x e^{-y^2}\, dy$$

and the subscript f designates the background field particles, ions, and electrons. The change in the parallel velocity due to this change in velocity Δv is then

$$\Delta v_{||} = \xi\, \Delta v,$$

where ξ is the pitch, the cosine of the pitch angle.

(ii) *Pitch Angle and Energy Scattering*

The change in the parallel velocity due to the pitch angle and energy scattering during Δt is

$$\Delta v_{||} = v\, \Delta\xi + \xi\, \Delta v.$$

The changes in the pitch and particle velocity given by Boozer and Kuo-Petravic [22] are

$$\Delta\xi = -\nu\, \Delta t\, \xi + \delta_1[(1-\xi^2)\, \nu\, \Delta t]^{1/2}$$

$$\Delta v = \left[v^2 + \frac{2}{m}\Delta E\right]^{1/2} - v,$$

where

$$\Delta E = -2\nu_E\, \Delta t\left[E - \left(\frac{3}{2} + \frac{E}{\nu_E}\frac{d\nu_E}{dE}\right) T\right] + \delta_2[4TE(\nu_E\, \Delta t)]^{1/2}.$$

Both δ_1 and δ_2 are ± 1 with equal probabilities, T is the background Maxwellian temperature, and the Spitzer collision frequencies [23] are

$$\nu = \frac{1}{2v^3}\sum_f C_f[\phi(l_f v) - G(l_f v)]$$

$$\nu_E = \frac{1}{v^3}\sum_f [C_f\, G(l_f v)(l_f v)^2].$$

(iii) *ICRF Interaction*

Each time the ion passes through the ion cyclotron resonance layer and undergoes resonant interaction with the wave field there is a random change in the perpendicular component of the particle velocity. To take into account this incremental change we use a method based upon the simplified treatment of Stix [21],

$$\Delta v_\perp = \frac{q}{2m}\tau\, |E_+|\, e^{-LZ^2} g(Z)\, e^{i\alpha}\left[J_{n-1}\left(\frac{k_\perp v_\perp}{\omega_{ci}}\right) + \frac{E_-}{E_+} J_{n+1}\left(\frac{k_\perp v_\perp}{\omega_{ci}}\right)\right](1 - k_{||} v_{||}/\omega),$$

where E is the electric field strength with + and − designating the polarized left- and right-handed components, respectively, L is the electric field profile parameter, Z is the distance from the median plane in the vertical direction, and $g(Z)$ is a function which is used to provide a flat power absorption profile when $L = 0$. J_n is the usual Bessel function of order n; $k_\perp$ and $k_{||}$ are the perpendicular and parallel wave numbers, respectively, ω is the radio frequency, and the phase angle is

$$\alpha = 2\pi\delta_3,$$

where δ_3 is a uniformly distributed random number between 0 and 1. For the passing and weakly trapped particles the resonance duration time τ is

$$\tau = \left[2\pi \Big/ \left(\frac{q}{m} v_{||} \frac{\partial B}{\partial s}\right)\right]^{1/2},$$

and when the orbit turning point is on or near the resonance layer we take

$$\tau = \left(2\pi \Big/ \left[\frac{q}{2m^2}\mu\left(\frac{\partial B}{\partial s}\right)^2\right]^{1/3}\right) A_i(0),$$

where A_i is the Airy function, and s is the distance along the particle trajectory. The ICRF induced diffusion is taken into account by calculating the change in the parallel velocity component [21]

$$\Delta v_{||} = \frac{k_{||}}{n\omega_{ci}} v_\perp\, \Delta v_\perp,$$

which in addition leads to spatial diffusion [24, 25]. The change in the particle velocity is then obtained from

$$\Delta v = [v^2 + 2\,|\Delta v_\perp|\, v_\perp \cos\alpha + 2v_{||}\, \Delta v_{||} + |\Delta v_\perp|^2 + (\Delta v_{||})^2]^{1/2} - v.$$

(iv) *Acceleration of Scattering Processes*

To achieve acceptable computing time an enhanced acceleration of the slowing down and scattering processes

has to be introduced. Goldston *et al.* coupled the acceleration to the change in pitch $\langle \Delta\xi \rangle$ with a predetermined acceleration constant G [10]. The acceleration was reduced by a factor of 2 when the change in pitch is above the upper limit G and increased by the same factor below the lower limit $0.5^{1/2}G$. To improve statistics in HECTOR the increase/decrease factor of 1.25 and the lower limit of $0.5G$ are used. Typically G can be 0.05–0.08, but higher values will lead to increased scattering losses due to enhanced change from passing orbits to trapped ones.

When velocity increases the reduction in the scattering frequency occurs at a faster rate than that in the timestep $\Delta t \sim \Delta s/v$. Thus, to prevent an excessive growth in acceleration, which would lead to a distorted slowing down and tail formation during ICRH, an upper limit for the acceleration is required. A fixed value upper limit is not efficient in view of CPU time, and thus, a scaling factor $(v/v_{th})^{1/2}$ is added during slowing down calculations. When the ICRH is on, to improve the statistics near the axis where the particle–wave field is the strongest, the acceleration is, in addition, scaled with $[1 + a(1 - e^{-LZ^2})]$. Typically acceleration of the order of 20 and the constant a value of 2 are used. To reduce the large computation time spent on the thermal population further, a cutoff energy of $10^{-4}T_i(0)$ is adopted.

IV. CALCULATIONS OF SOURCE FUNCTION AND PLASMA QUANTITIES

The application of direct sampling methods to the problem of particle selection from the distribution of sources in the local phase space coordinates leads to orbit duplication, and many repetitions of the same equivalent particle occurs. Consequently, a very large number of particles will have to be traced to obtain good statistical accuracy. To circumvent this difficulty, we note that particles produced in different regions of phase space are simply connected through unique sets of $(P = P_\phi, \mu, v)$ coordinates. Each set is common to all particles born along a particular orbit and can be represented by a single test particle. The point on the path at which the test particle is initially located is usually taken to be the median plane of the torus but is otherwise quite arbitrary. In this way, a transformation to the COM phase space will lead to a significant reduction in the number of charged particles that have to be tracked to ensure that sampling errors are minimised. It is to be noted that the reduction in the number of test particles does not only apply to orbits where the drag term dominates but also to those of ICRF heated particles. The history of a particular particle during ICRH follows the same pattern from thermal to strongly anisotropic with a high tail temperature, leading to diffusion out of the plasma centre and, after cooling, returning due to diffusion back into the centre for reheating. The orbit integrated source function in the local velocity space variables (R, Z, v, ξ) is transferred to the COM system (P, μ, v), where the local source strength is given by

$$S = 4\pi^2 \iiiint S(R, Z, v, \xi)\, R\, dR\, dZ\, v^2\, dv\, d\xi.$$

For charged particles resulting from thermonuclear reactions within the plasma the local source function takes the form

$$S(R, Z, v, \xi) = \frac{n_1 n_2 \langle \sigma v \rangle}{4\pi v_0^2} \cdot \delta(v - v_0),$$

where $\langle \sigma v \rangle$ is the thermonuclear reactivity, v_0 is the birth velocity, and the particles are assumed to be born isotropically in velocity space. The local birth rate of fast neutral beam particles is described with

$$\dot{n} = (\dot{n}_o - \dot{n}_e)(1 - x^a)^b + \dot{n}_e,$$

where the subscripts (o, e) refer to the values on the magnetic axis and at the plasma edge, respectively, and (a, b) are the profile parameters. The initial pitch of the beam particles is assumed to have a narrow Gaussian distribution and is related to the magnetic field configuration and the beam line geometry.

The distribution function for the test particle species can be constructed by integrating over the local phase space coordinates along the orbits and by weighting the particle flights with the appropriate source terms. However, quantities of interest, such as the rates of the background heating and ICRF power absorption, and thermonuclear yields, can be obtained directly from the orbit integration and do not require a detailed knowledge of the test particle distribution function. Thermonuclear yields are calculated by integrating the hot target reactivity $\langle \sigma v \rangle_h$ [26], and the burnup fraction is then

$$\rho = \frac{\sum_k N_{ok}[1 - \pi(1 - \langle \sigma v \rangle_h n\, \Delta t)_i]}{\sum_k N_{ok}},$$

where N_{ok} is the number of test particles, and n is the target density. Index i refers to the integration steps along the orbit.

V. INPUT DATA

Tracing charged particles requires a continuous supply of local values of magnetic field and bulk plasma parameters along the particle trajectory. Two equidistant (but not limited to) spatial grids are used to facilitate an easy access to these values.

The radial density and temperature profiles of the plasma electrons, primary ions, and impurity ions, and the calculated profiles of thermonuclear reactivities and other cross sections of interest are stored in 51 grid points. The values of the magnetic field components B_R, B_ϕ, B_z, magnitude of the field $|\mathbf{B}|$, flux coordinate ρ, poloidal flux function ψ, and reference coordinates of the 1D grid are precalculated and stored in a 2D grid spanning the entire poloidal cross section of the torus. To obtain particular values and to reduce the computational time still further and, furthermore, to avoid a recourse to interpolation, we employ a simple "look-up" table procedure. Unfortunately, this procedure demands a fine grid, resulting in a considerable increase in storage requirements. However, a (200×299) grid was found to give acceptable results. The input data can be divided into two categories, depending on whether model or arbitrary values and profiles (model input data) or data from JET discharges (JET shot input data) are used.

(i) *Model Input Data*

In this mode the code can be used with a wide variety of input parameters appropriate to other tokamaks in addition to JET. The model profiles for the electron and ion densities and temperatures are

$$n_j = (n_{jo} - n_{je})(1 - x^2)^a + n_{je}$$
$$T_j = (T_{jo} - T_{je})(1 - x^2)^b + T_{ie}, \quad j = (i, e).$$

The constants a, b, and c are the usual profile parameters. Furthermore, arbitrary profiles can be created with separate input data points.

The toroidal component of the magnetic field is calculated from

$$B_\phi = B_o R_o / R,$$

where B_o is the toroidal magnetic field at $R = R_o$.

The poloidal magnetic field B_θ is derived from the Lao–Hirshman solution of the Grad–Shafranov equation for the plasma equilibria and assumes an analytical representation for the plasma current and pressure profiles [27]. The model has been corrected to satisfy $\nabla \cdot \mathbf{B} = 0$ [26]. Both symmetric and non-symmetric plasma cross sections can be included. The input parameters for the B_θ calculations are: plasma current, current profile constant, beta-i, elongation, internal inductance, and minor radius. In the hybrid method the value of the poloidal flux ψ is required, and this is obtained by integrating over the median plane the equation

$$\frac{\partial \psi}{\partial R} = B_\theta R.$$

(ii) *JET Shot Input Data*

To obtain the poloidal flux function ψ the code IDENTC is used [28]. The code solves the Grad–Shafranov equation for plasma equilibria assuming an analytical representation of the current and pressure profiles and using free parameters to fit the data from the magnetic measurements. The output is a normalized ψ between 0 and 1.

The FLUSH routine package [29] is then used to calculate the actual values of ψ, and the poloidal magnetic field components B_R and B_z at given coordinates.

Routine PREGER [30] is used to extract data, such as n_e, T_e profiles, from JET shot data banks. Densities for the primary and impurity ions are then calculated using the CPRIO routine [30], which employs the coronal equilibrium model. The local birth rate of the fast neutral beam particles can be included by fitting the data from the PENCIL code [31].

VI. TEST RESULTS

An extensive program of tests was carried out to assess the reliability and accuracy of HECTOR. The comparison with the SOCRATE code [16], which combines the single orbit approximation with the classical energy loss formula, showed a very good agreement in the orbit topology, the source rate, the slowing down rate, and the triton burnup (Table I) [19].

TABLE I

Triton Burn up and Confined Particle Fraction Calculated with HECTOR and SOCRATE Codes

	Shot: 10583				Shot: 10952			
	Flat profile		Peaked profile		Flat profile		Peaked profile	
	HECTOR	SOCRATE	HECTOR	SOCRATE	HECTOR	SOCRATE	HECTOR	SOCRATE
p(%)	0.50	0.50	0.74	0.79	1.29	1.31	1.54	1.62
f_c(%)	50	49	93	94	70	69	100	100

Note. The effects of pitch angle scattering and energy diffusion are not included.

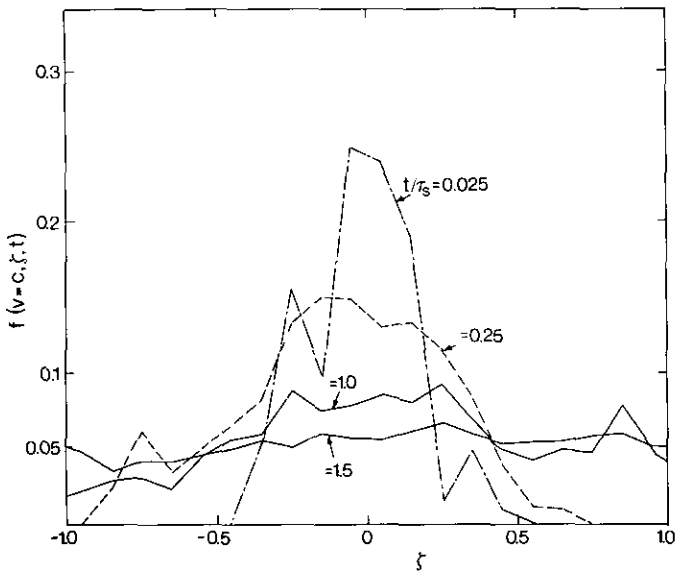

FIG. 4. Particle relaxation in pitch space. A single, thermal $E = T$, ^{3}He ion was followed with the pitch angle scattering operator in deuterium plasma. The particle started with an initial pitch $\xi = 0.0$, and after 1.5 Spitzer time isotropic pitch distribution was obtained.

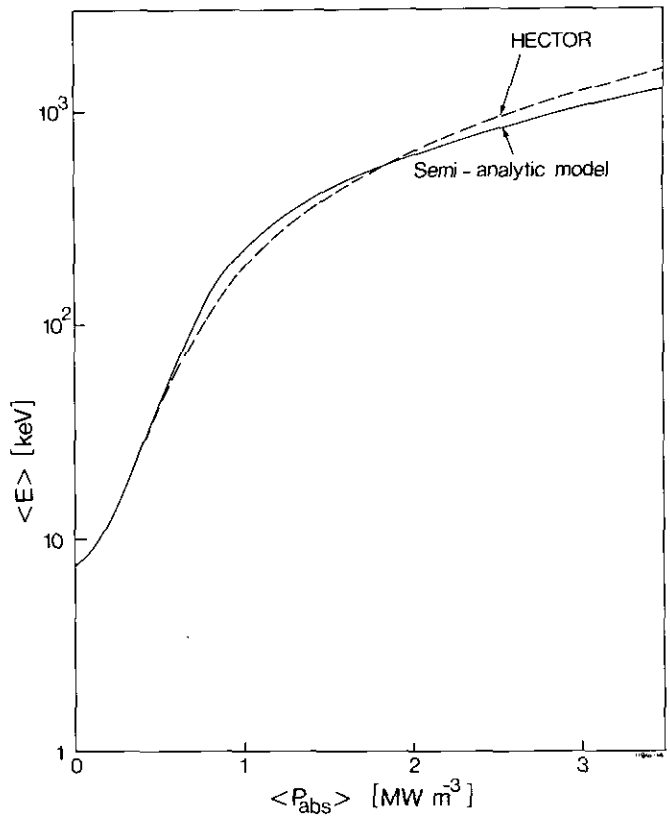

FIG. 6. Comparison of the mean energy calculated with the Fokker–Planck and HECTOR codes. The parameters for the calculation are $I_p = 5MA$, $B_\phi = 3.4T$, $T_e = 8$ keV, $n_e = 5 \times 10^{19}$ m^{-3}, and $Z_{\text{eff}} = 1.2$.

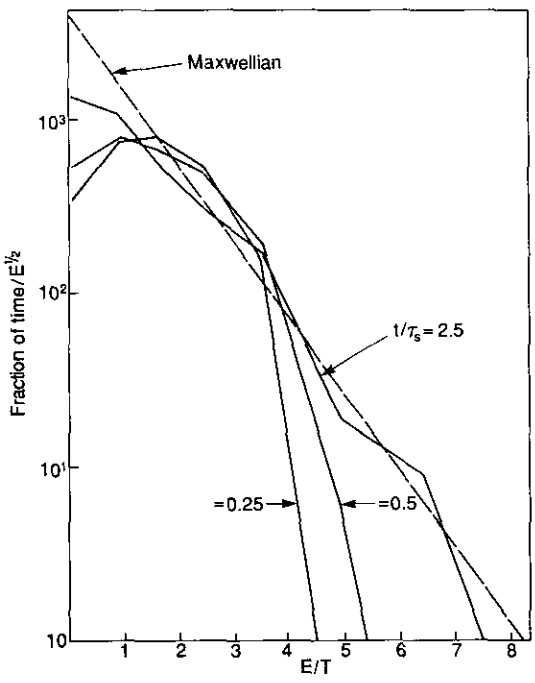

FIG. 5. Particle relaxation in energy space. A ^{3}He ion was followed with the energy scattering operator in deuterium plasma. The initial energy was $E = T$. A Maxwellian distribution, represented with the straight line, is reached after 2.5 Spritzer time. A cutoff energy of $E = 10^{-4}T$ was used.

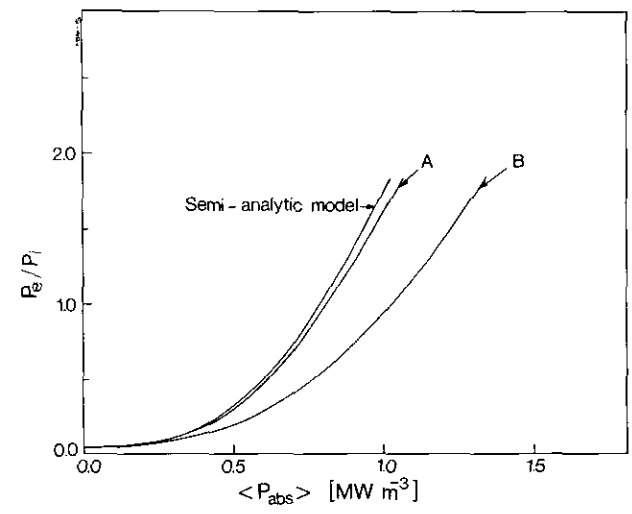

FIG. 7. Comparison of the electron and background ion heating rates calculated with the Fokker–Planck and HECTOR codes. In case A the effect of the particle losses out of the plasma is not included, but in case B it is. The parameters for the calculation are $I_p = 5MA$, $B_\phi = 3.4T$, $T_e = 8$ keV, $n_e = 5 \times 10^{19}$ m^{-3}, and $Z_{\text{eff}} = 1.2$.

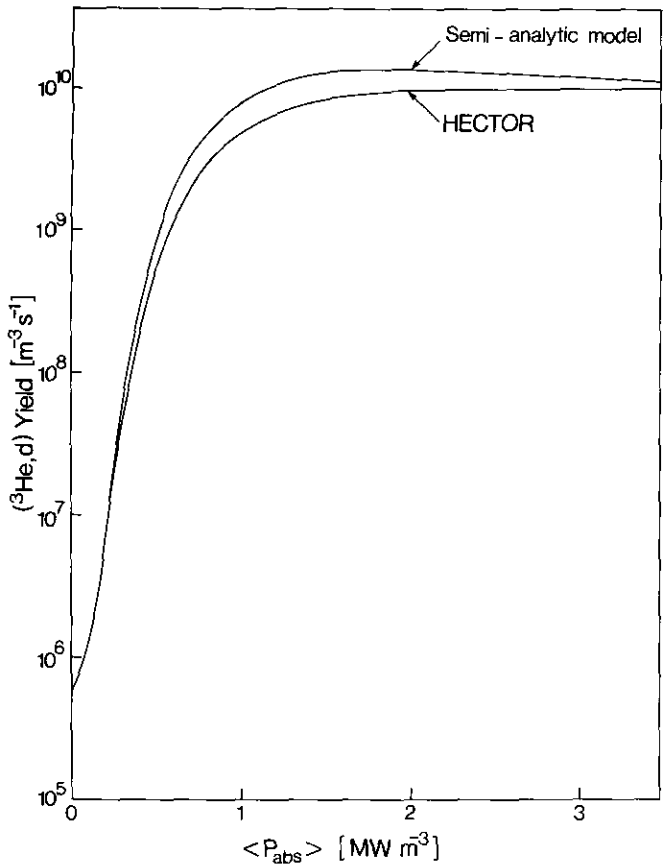

FIG. 8. Comparison of the (^{3}He, d) yield calculated with the Fokker–Planck and HECTOR codes. Flat plasma and ICRF wave field provides were used to eliminate the finite orbit effects in HECTOR. The parameters for the calculation are $I_p = 5MA$, $B_\phi = 3.4T$, $T_e = 8$ keV, $n_e = 5 \times 10^{19}$ m^{-3}, and $Z_{eff} = 1.2$.

The spread in pitch for a single thermal ^{3}He-particle behaved as expected and in the JET deuterium plasma reached a uniform distribution after several collision times (Fig. 4). Furthermore, the diffusion coefficient and the consequent particle losses were within 10% of the neoclassical values. Separate tests of the energy diffusion operator showed that the energy relaxation of a thermal ^{3}He-particle reached the Maxwellian distribution in a time scale that was longer than that for the pitch relaxation (Fig. 5).

The validity of the ICRF interaction model was tested by comparing it with a semi-analytical model [32] which is in good agreement with the bounced-averaged Fokker–Planck ion cyclotron code BAFIC [33]. To eliminate the finite orbit effects in the results, flat profiles for the ICRF wave fields and plasma parameters were used. The minority ion energy content, mean energy (Fig. 6), energy transferred to background electrons and ions (Fig. 7), and the fusion yield (Fig. 8) are in good agreement (within 10%), when particle losses are taken into account.

VII. CONCLUDING REMARKS

The new numerical technique for integrating the charged particle orbits, together with a fine 2D spatial grid and its corresponding 1D grid for easy data handling, have reduced the computation time for each particle flight. Introducing the orbit integrated source rate has reduced significantly the number of particle orbits that have to be traced. A simulation following 2000 test particles for a Spitzer time takes, depending on the application, 10–20 min CPU time on the IBM-3090-300J computer. The time evolution of the plasma parameters can be taken into account but this will increase the CPU time and space requirement. In most applications the assumption of the steady state plasma is sufficient.

ACKNOWLEDGMENTS

We thank A. Taroni, C. Sack, and E. Springmann for providing program modules TRESCO, DBGET, PREGER, CPRIO, FLUSH, and FLUPNG for the JET shot data input mode, and P. van Belle and G. Sadler for providing program modules for full orbit calculations, including the poloidal field presentation for the model input mode and the routine for the triton hot target reactivity. We also appreciate fruitful discussions with H. Hamnén and T. Hellsten and help from the JET Data Management Group. M. A. Kovanen is grateful to JET Theory Division for hospitality and to the Finnish Cultural Foundation and to Jenny and Antti Wihuri's Foundation for financial support.

REFERENCES

1. R. Dei-Cas and D. Marty, Fontenay-aux-Roses Report EUR-CEA-FC-726, 1974 (unpublished).
2. M. Ohnishi, J. Tokunaga, and J. Wakabayashi, *Nucl. Fusion* **16**, 693 (1976).
3. D. L. Jassby and R. J. Goldston, *Nucl. Fusion* **16**, 613 (1976).
4. G. G. G. Lister, D. E. Post, and R. J. Goldston, in *Proceedings, 3rd Varenna Symposium on Plasma Heating in Toroidal Devices, Bologna, Italy, 1976*, p. 303.
5. T. W. Petrie and G. H. Miley, *Nucl. Sci. Eng.* **64**, 151 (1977).
6. M. Ohnishi, N. Ao, and J. Wakabayashi, *Nucl. Fusion* **18**, 859 (1978).
7. W. Bauer, K. L. Wilson, C. L. Bisson, L. G. Haggmark, and R. J. Goldston, *Nucl. Fusion* **19**, 93 (1979).
8. D. R. Mikkelsen and D. E. Post, in *Proceedings, Sherwood Conference on Theoretical Aspects of Controlled Thermonuclear Fusion, Mt. Pocono, 1979*, p. 1B21.
9. R. H. Fowler and J. A. Rome, Oak Ridge National Lab. Report ORNL/TM-7774, 1981 (unpublished).
10. R. J. Goldston, D. C. McCune, H. H. Towner, S. L. Davis, R. J. Hawryluk, and G. L. Schmidt, *J. Comput. Phys.* **43**, 61 (1981).
11. B. Gagey, Y. Lapierre, and D. Marty, in *Proceedings, 3rd Joint Varenna–Grenoble Int. Symposium on Heating in Toroidal Plasmas, Grenoble, France, 1982*, p. 361.
12. K. Tani, T. Takizuka, M. Azumi, and H. Kishimoto, *Nucl. Fusion* **23**, 657 (1983).
13. K. W. Whang and G. J. Morales, *Nucl. Fusion* **23**, 481 (1983).
14. L. M. Hively, *Nucl. Fusion* **24**, 779 (1984).

15. G. G. Lister, Max-Planck-Institut für Plasmaphysik Report IPP 4/222, 1985 (unpublished).
16. E. Bittoni and M. Haegi, Ass. EURATOM ENEA Sulla Fusione CRE-FRASCATI Report RT-FUS-86-13, 1986 (unpublished).
17. L. M. Hively, G. H. Miley, and J. A. Rome, *Nucl. Fusion* **21**, 1431 (1981).
18. G. Gorini and M. A. Kovanen, JET Joint Undertaking Report JET-R(88)09, 1988 (unpublished).
19. G. Hall and J. M. Watt (Eds.), *Modern Numerical Methods for Ordinary Differential Equations* (Clarendon Press, Oxford, 1976).
20. W. D. D'Haeseleer, in *Proceedings, 17th EPS Conference on Controlled Fusion and Plasma Physics, Amsterdam, 1990*, p. 748.
21. T. H. Stix, *Nucl. Fusion* **15**, 737 (1975).
22. A. H. Boozer and G. Kuo-Petravic, *Phys. Fluids* **24**, 851 (1981).
23. L. Spritzer, Jr., *The Physics of Fully Ionized Gases*, 2nd rev. ed. (Interscience, New York, 1962).
24. S. Riyopoulos, T. Tajima, T. Hatori, and D. Pfirsch, *Nucl. Fusion* **26**, 627 (1986).
25. L. Chen, J. Vaclavic, and G. W. Hammett, *Nucl. Fusion* **28**, 389 (1988).
26. P. Van Belle and G. Sadler, JET Joint Undertaking, private communication (1986).
27. T. E. Stringer, JET Joint Undertaking Report JDN/T(83)6, 1983 (unpublished).
28. E. Lazzaro and P. Mantica, *Plasma Phys. Controlled Fusion* **30**, 1735 (1988).
29. E. M. Springmann, JET Joint Undertaking, private communication (1988).
30. H. C. Sack and E. M. Springmann, JET Joint Undertaking, private communication (1988).
31. P. M. Stubberfield and M. L. Watkins, JET Joint Undertaking Report DPA(06)/87, 1987 (unpublished).
32. D. Anderson, W. G. F. Core, L.-G. Eriksson, H. Hamnén, T. Hellsten, and M. Lisak, *Nucl. Fusion* **27**, 911 (1987).
33. S. Succi, K. Appert, W. G. F. Core, H. Hamnén, T. Hellsten, and J. Vaclavik, *Comput. Phys. Commun.* **40**, 137 (1986).